

# Preparation and Characterization of Cellulose Nanofiltration Membrane Through Hydrolysis Followed by Carboxymethylation

Rengui Weng<sup>1,2</sup>, Lihui Chen<sup>1\*</sup>, He Xiao<sup>1</sup>, Fang Huang<sup>1</sup>, Shan Lin<sup>1</sup>, Shilin Cao<sup>1</sup>, and Liulian Huang<sup>1</sup>

<sup>1</sup>College of Material Engineering, Fujian Agriculture and Forestry University, Fuzhou, Fujian 350002, China

<sup>2</sup>College of Ecological Environment and Urban Construction, Fujian University of Technology, Fuzhou 350118, China

(Received March 6, 2017; Revised May 1, 2017; Accepted May 7, 2017)

**Abstract:** Bamboo cellulose (BC) is hydrophilic, biodegradable and inexhaustible. The bamboo cellulose membrane (BCM) is one of the best materials to replace petroleum-based polymer film for water purification. In this study, the N-methylmorpholine-N-oxide (NMMO) was used as a solvent to dissolve cellulose 6 wt.%, and regenerated cellulose membrane was prepared by phase inversion. A new kind of cellulose nanofiltration membrane (BC-NFM) was obtained by the hydrolysis and carboxymethylation of dense cellulose membrane (BCM). The modification was carried out through hydrolysis followed by carboxymethylation. The BC-NFM was characterized by XRD, FT-IR, SEM and thermal analysis. BC-NFM performance evaluation instrument were used to evaluate retention rate and water flux of nanofiltration membrane. BCM was immersed in 1 mol/l NaOH and 3 wt/v.% chloroacetic acid solution to obtain BC-NFM. By calculating, pore size of nanofiltration membrane was 0.63 nm. With a pressure of 0.5 MPa, the water flux of nanofiltration membrane for Na<sub>2</sub>SO<sub>4</sub> solution was 10.32 l/m<sup>2</sup>h, and the retention rate was 68.4 %. The water flux for NaCl solution was 13.12 l/m<sup>2</sup>h, and the retention rate was 34.9 %. And the retention rates were 93.0 % and 98.9 % for methyl orange and methyl blue, respectively. The stability of the nanofiltration membrane was measured by the thermal analyzer, following the order of BC > BCM > BC-NFM. The prepared cellulose nanofiltration membrane exhibited good stability in water treatment process, and can be used to remove organic compounds in aqueous solutions.

**Keywords:** Bamboo cellulose, Nanofiltration membrane, Hydrolysis, Carboxymethylation

## Introduction

Nanofiltration membrane is developed from reverse osmosis membrane. It is between reverse osmosis membrane and ultrafiltration membrane in separation performance [1,2]. Due to its ability to separate low-molecular-weight organic species and metal ions, it has become an important separation and purification technique in the wastewater reclamation, separation of substances, and so on [3-5]. At present most nanofiltration membranes are prepared with non-biodegradable petrochemical materials, polyethersulfone (PES) and polyvinylidene fluoride (PVDF) membranes are mostly sold as microfiltration or ultrafiltration membranes, and they usually require further modifications to behavior like NF membranes. Prepared PES nanofiltration membranes by blending negatively charged surface modifying macromolecule (CSMM) in the spinning formulation through the phase-inversion technique [6]. It was reported that PES nanofiltration membrane with a mean pore size of about 1.2 nm in diameter could be tailor-made and used to remove the bisphenol A (BPA) from aqueous solution effectively. Fabricated polysulfone nanofiltration hollow fiber membranes through UV-photografting process was in their outer surface [7]. The diallyl dimethyl ammonium chloride was grafted onto the surface: so it becomes hydrophilic and positively charged, pore-size is reduced. The membrane permeability was reduced and high retentions of the calcium ion were obtained even though the MWCO remained high. Prepared PVDF nanofiltration

membranes were fabricated through interfacial polymerization. The membranes were prepared on the support of PVDF ultrafiltration membranes with piperazine (PIP) as aqueous monomer and trimesoylchloride (TMC) as organic monomer [8]. More recently, composite capillary membrane for solvent resistant nanofiltration was developed through coating a selective poly(dimethylsiloxane) (PDMS) top layer on an  $\alpha$ -alumina support [9]. However, these non-biodegradable petrochemical materials lead to energy waste and destruction of the ecological environment. So developing an environmentally friendly biodegradable membrane has great significance for the ecological environment.

It is vital to find ideal materials to replace petroleum-based materials for membrane production. Cellulose is one of the most abundant renewable, biodegradable and inexpensive organic materials and considered as an environmentally friendly and biocompatible product [10,11]. As we know, cellulose molecules have very strong hydrogen bonds between each other because of polyhydroxy feature of cellulose. Therefore, cellulose can not be directly processed into membrane. There are two methods of processing cellulose into membrane, the first approach is to made cellulose into derivatives such as cellulose ether, and ester, then the derivatives are used to prepare cellulose derivative membrane. The second approach is to dissolve cellulose in a solvent for preparing regenerated cellulose membrane [12]. Selecting the appropriate solvent is the key to prepare cellulose membrane. Up to date, only a limited number of solvent systems that readily dissolve cellulose have been found for manufacturing cellulose materials, such as DMAC/LiCl

\*Corresponding author: fafuclh@163.com

[13,14], NMP/LiCl [15], DMSO/paraformaldehyde [16,17] and LiSCN<sub>2</sub>H<sub>2</sub>O [18]. However, those traditional dissolution processes are facing many challenges because of high cost, the toxicity or difficulty for solvent recovery. In recent years, a number of new cellulose solvents have been developed, including of NMMO [19] and ionic liquids [20]. NMMO is safe, non-toxic, and has non-polluting production process, and can be reused efficiently, so in this study, NMMO solvent is used to dissolve cellulose for preparing regenerated cellulose membrane. The dissolution mechanism of cellulose in NMMO is direct dissolution, which is carried out by breaking the hydrogen bonds between cellulose molecules and there is no cellulose derivative. The BCM was prepared by the phase-inversion method with NMMO as the solvent of cellulose. The method can be used to prepare a complete and dense cellulose membrane with no defect.

Nanofiltration membrane has attracted more attentions in recent years. Cellulose acetate reverse osmosis membrane was fabricated to prepare nanofiltration membrane by modification [21]. In recent years, NMMO as a solvent mainly focused on the cellulose ultrafiltration membrane, blend membrane, and microspheres [22,23]. Li *et al.* [24] prepared high-flux and anti-fouling cellulose nanofiltration membranes with ionic liquid as solvent. However the membranes must be kept in water to avoid curling. So far, the regenerated cellulose nanofiltration membrane has been reported rarely, especially there have been no reports on cellulose nanofiltration membrane obtained by hydrolysis and carboxymethylation.

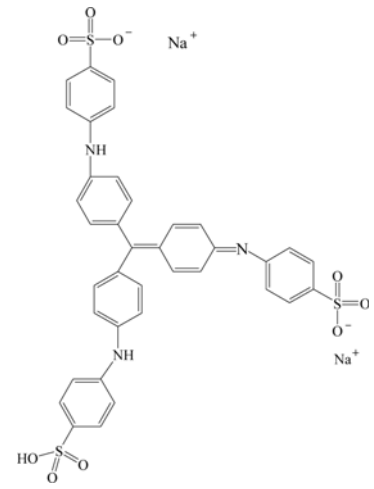
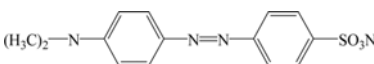
In this study, a new method of regenerated cellulose nanofiltration membrane was developed, which is simple and environmental friendly. The cellulose was dissolved in NMMO and coated on the non-woven fabric, the BCM was obtained by rinsing with water and drying, and BC-NFM was obtained by hydrolysis and carboxymethyl modification. The BC-NFM was characterized in terms of chemical composition, crystalline structure, thermal stabilities, and microstructure by FT-IR, XRD, Thermogravimetric analysis (TGA), SEM, respectively. The modification conditions were also studied. Dye removal tests were also conducted to demonstrate the improved permselectivity of the modified BCM. This research explores the chemical and physical properties, permeation and rejection of nanofiltration membrane.

## Experimental

### Materials

The bamboo cellulose (BC) with a polymerization degree of 650 was kindly provided by Sichuan Tianzhu Bamboo Resources Development Co. Ltd. (Sichuan, China). The BC was dried over night at 60 °C prior to dissolution. NMMO (AR, >97 %) was obtained from Tianjin Hainachuan Science and Technology Development Co., Ltd. Polyethylene glycol (PEG) ( $M_w=400, 600, 800, 1000$  and 2000 Da), propyl

**Table 1.** Characteristics of molecular dyes

Dye name	Molecular structure	$M_w$ (g/mol)	$\lambda_{max}$ (nm)
Methyl Blue		799.80	591
Methyl Orange		327.33	504

gallate, methyl orange and methyl blue dyes were purchased from Aladdin Chemical Regent Co., Ltd., China. The characteristics of two reactive dyes used in this study are listed in Table 1. The water used in this experiment is de-ionized water.

### Preparation of Cellulose Nanofiltration Membranes

The BC solution was prepared by dissolving a certain amount of cellulose powder in 86.7 % NMMO aqueous solution in a flask, and the mixture was heated at 110 °C and stirred until BC samples were completely dissolved. BC/NMMO solution with BC concentration of 6 wt.% was obtained. The PET non-woven fabric was fixed onto a glass plate of coater (GBC-A4, GIST, Korea). The solution was poured onto non-woven fabric and moved the roll at speed of 20 mm/s. The membrane was immersed in water coagulation bath at room temperature. Then the membrane washed with water to remove residual solvent. Finally, the membrane was air-dried at room temperature to obtain dense BCM.

In order to obtain BC-NFM, BCM was modified by hydrolysis and carboxymethylation. Firstly, hydrolysis was carried out by treating the BCM at 30 °C in 1 mol/l NaOH solution for 30 min. After that, the treated BCM was washed with water. Secondly, carboxymethylation was performed by treating the above hydrolyzed BCM at 60 °C chloroacetic acid and NaOH ( $n_{NaOH}:n_{Chloroacetic\ acid}=2.5:1$ ) mixture water solution. The carboxymethylated membrane was then washed with water and stored [21]. Preparation of BC-NFM through hydrolysis followed by carboxymethylation as schematically shown in Figure 1.

Mechanism of hydrolysis and carboxymethylation, firstly

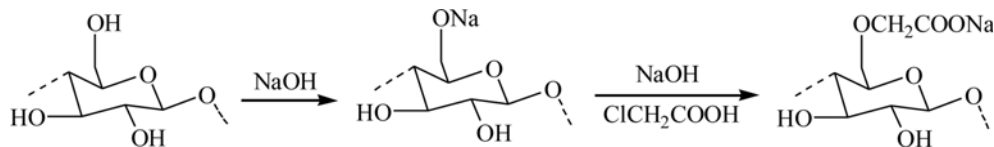


**Figure 1.** Hydrolysis and carboxymethylation of dense BCM.

the reaction of cellulose with sodiumhydroxide to form an alkali cellulose, be called alkalization reaction, secondly the reaction of alkali cellulose with chloroacetic acid to form carboxymethylcellulose, be called etherification reaction.

### Characterization of Cellulose Nanofiltration Membrane

The cellulose powder, BCM and BC-NFM were tested by Fourier transforms infrared spectroscopy (FT-IR). The spectra with a wave number ranging from  $4000\text{ cm}^{-1}$  to  $400\text{ cm}^{-1}$  were recorded on a Fourier Transform Infrared spectrometer (Thermo Nicolet 380) by the KBr-disk method.

The surface and cross-sectional morphology of BCM and BC-NFM were investigated with a FEI Nova NanoSEM450 field emission scanning electron microscopy (FE-SEM). The samples were freeze-fractured in liquid nitrogen, followed by sputtering with gold in a sputtering device.

The crystal structures were analyzed by X-ray diffraction (XRD). The XRD measurements were carried out by a reflection method on a MiniFlex2 XRD diffractometer (Japan Rigaku) with a Cu K-radiation of  $1.54\text{ \AA}$  at 40 kV and 30 mA. The patterns were performed in the region of  $2\theta$  range from  $5^\circ$  to  $60^\circ$ .

The material mass losses relationship with change of temperature was determined with a TG-DTA instrument (Netzsch STA 449 F3) at the heating rate of  $10^\circ\text{C}/\text{min}$  under nitrogen with a flow rate of  $20\text{ ml}/\text{min}$ . Each sample was weighed about 2 to 3 mg as a standard and heated from  $30^\circ\text{C}$  to  $600^\circ\text{C}$ .

### Cross-flow Permeation Tests

Membrane permeation tests were performed at an operating pressure using a flat-sheet cross-flow permeation test cell with membrane area of  $50.24\text{ cm}^2$ . The equipment used for membranes performance evaluation is shown in Figure 2. All the membranes loaded in the equipment were pressured with water under 0.5 MPa for at least 30 min

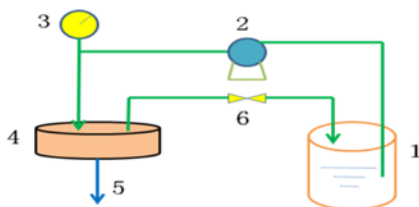


**Figure 2.** Membrane performance evaluation instrument; (1) feed tank, (2) pump, (3) pressure gauge, (4) membrane cell, (5) permeate, and (6) valve.

before testing to get stable membrane water flux.

The permeation flux of membrane was calculated using the following equation.

$$J = V/(A \times t) \quad (1)$$

where  $J$  is the permeation flux ( $\text{l}/\text{m}^2\text{h}$ ),  $V$  is the permeate volume (L),  $A$  is the membrane area ( $\text{m}^2$ ), and  $t$  is the permeation time (h).

A conductivity meter (STARTER 3100C, USA) was used to determine solute concentrations in the permeate and feed. The dye concentration was measured using a UV-visible spectrophotometer (Agilent 8453, USA) at the maximal absorption wavelength of each organic dye. The membrane rejection rate ( $R$ ) of the dye or salt was calculated as follows:

$$R = 100\% \times (C_f - C_p)/C_f \quad (2)$$

where  $R$  is the rejection rate (%),  $C_f$  is the feed concentration ( $\text{mg}/\text{l}$ ), and  $C_p$  is the permeate concentration ( $\text{mg}/\text{l}$ ). All experiments of cross-flow permeation were completed at room temperature.

### Characterization of Molecular Weight Cut-off and Mean Pore Size

The molecular weight cut-off (MWCO) value is taken by the molecular weight of PEG molecules that are rejected by the membrane to 90 % [25]. By measuring the retention rate of solutes of different molecular weights (usually PEG), one can obtain the relationship curve between the retention rate of the membrane and the molecular weight of the solute.

The experiment measures the retention performance of the solution to characterize the MWCO of the membrane by measuring PEGs of different molecular weights ( $M_w=400, 600, 800, 1000$  and  $2000\text{ Da}$ ).

The following holds, according to the Stokes-Einstein equation [26]:

$$r = 16.73 \times 10^{-3} \times M_w^{0.557} \quad (3)$$

where  $r$  is the Stokes Radius (nm), and  $M_w$  is the molecular weight of PEG(Da).

## Results and Discussion

### Structure Characterization of Membrane

The FT-IR spectra and characteristics absorption peaks of

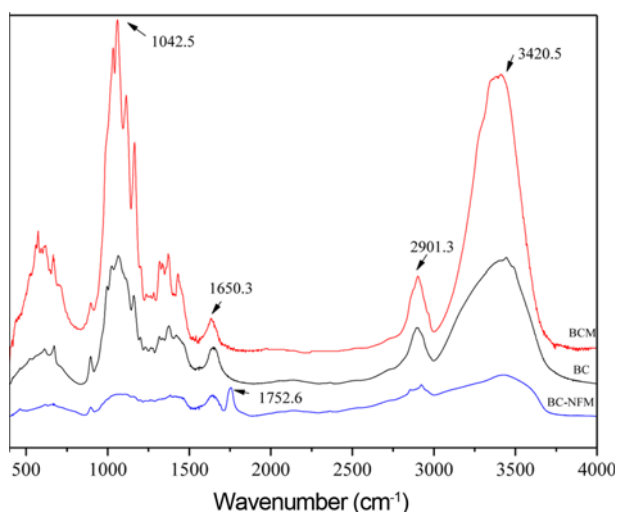


**Figure 3.** FTIR spectra of BC, BCM and BC-NFM.

the BC, BCM and BC-NFM were shown in Figure 3 and Table 2. In comparison spectra and data of BC, BCM, BC-NFM, it was showed that FTIR spectrum of BCM was similar to BC, which indicates that there was no significant difference in the structure of BC and BCM. Chemical reaction doesn't occur in the process of dissolution and coagulation bath of cellulose and it only had physical change, which shown that NMMO solution was non-derivatized solvent of cellulose. The results were similar to earlier reports using a blend of chitosan and cellulose in a solvent of  $ZnCl_2 \cdot 3H_2O$  [27]. The peak at  $1752.6\text{ cm}^{-1}$  arise from the  $C=O$  of carboxyl, present in BC-NFM, it showed that a part of hydroxyl in cellulose transforms to carboxymethyl during hydrolysis and carboxymethylation of BCM. The featured peak of  $-OH$  for BC-NFM is appreciably decreased, because the hydroxyl groups of the BCM has been partly substituted by carboxymethyl groups.

Figure 4 is XRD diffraction pattern of BC, BCM and BC-NFM. The XRD pattern of BC shows three diffraction peaks at  $2\theta=15.4^\circ, 22.6^\circ, 34.2^\circ$ , which originates from the cellulose crystalline plane (101), (002), (040) [28]. However, the diffraction pattern of the BCM and BC-NFM exhibit only a peak at  $2\theta=22.7^\circ$ , and no other peaks were observed, suggesting that during the dissolution and regeneration process of cellulose, the transformation of crystalline structure from cellulose I to cellulose II occurs [29]. In

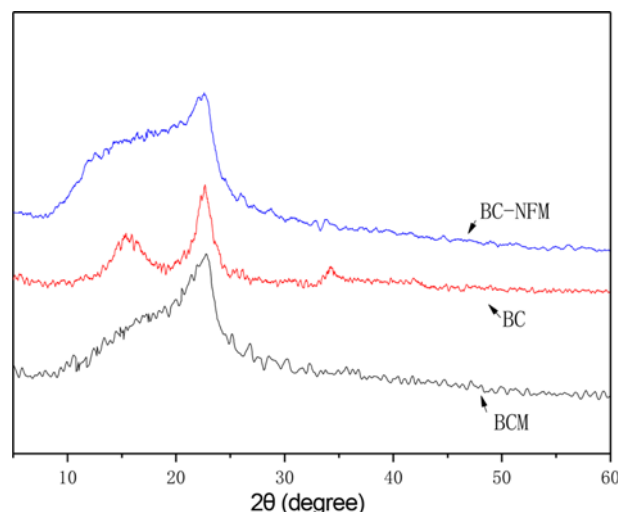


**Figure 4.** XRD diffraction pattern of BC and BCM.

addition, the crystallization degree of BCM and BC-NFM were lower than that of BC, but the native crystal structure of BC had not changed.

Thermal stabilities of the BC, BCM and BC-NFM were tested by TG-DTA analyzer in nitrogen atmosphere. The results were shown in the Figure 5 which initial decomposition temperature of BC, BCM and BC-NFM were  $298.4^\circ\text{C}$ ,  $271.3^\circ\text{C}$  and  $248.2^\circ\text{C}$ , respectively. The maximum decomposition rate happened at  $347.8^\circ\text{C}$ ,  $338.2^\circ\text{C}$  and  $321.5^\circ\text{C}$  respectively, which was due to dehydration, heat degradation of membrane and cellulose. The data of TG showed that before 32 min weight residues order was  $BC > BCM > BC-NFM$ , but after 32 min weight residues order was  $BC-NFM > BCM > BC$ . The thermal stability of regenerated cellulose was lower, because the hydrogen bonds between the cellulose were separated in the dissolution, but the hydrogen bonds of regenerated cellulose were not completely reconstructed. On the other hand, degree of polymerization of the regenerated cellulose declined, which also affected the thermal stability of BCM. The thermal stability of BC-NFM was lower than the BCM. This behavior may be explained by the binding force of bonds may be weakened after hydrogen bonds were opened.

The surface and cross-sectional microstructure of BCM and BC-NFM were characterized by FE-SEM (Figure 6). As observed from Figure 6(a), BCM is smooth and dense. No

**Table 2.** Characteristic absorption peaks of FTIR

	A	B	C	D	E	F	G
BC	3445.8	2902.2		1648.2	1424.4	1380.1	1046.7
BCM	3420.5	2901.3		1650.3	1429.9	1375.5	1042.5
BC-NFM	3438.2	2916.7	1752.6	1642.7	1430.9	1382.3	1050.2

A:  $-OH$  stretching, B:  $-CH$  stretching, C:  $C=O$  stretching of carboxyl, D:  $C=O$  stretching (amide I) and absorbed water in the amorphous region, E:  $-CH$  bending vibrations, F:  $-CH_3$  bending vibrations, G: Anti-symmetric stretching of the  $C-O-C$  bridge.

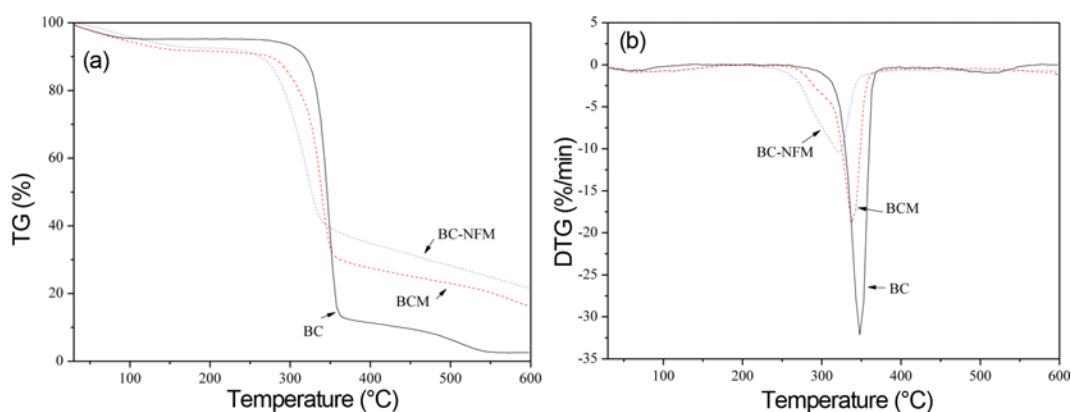


**Figure 5.** TG and DTG analysis of BC, BCM and BC-NFM.

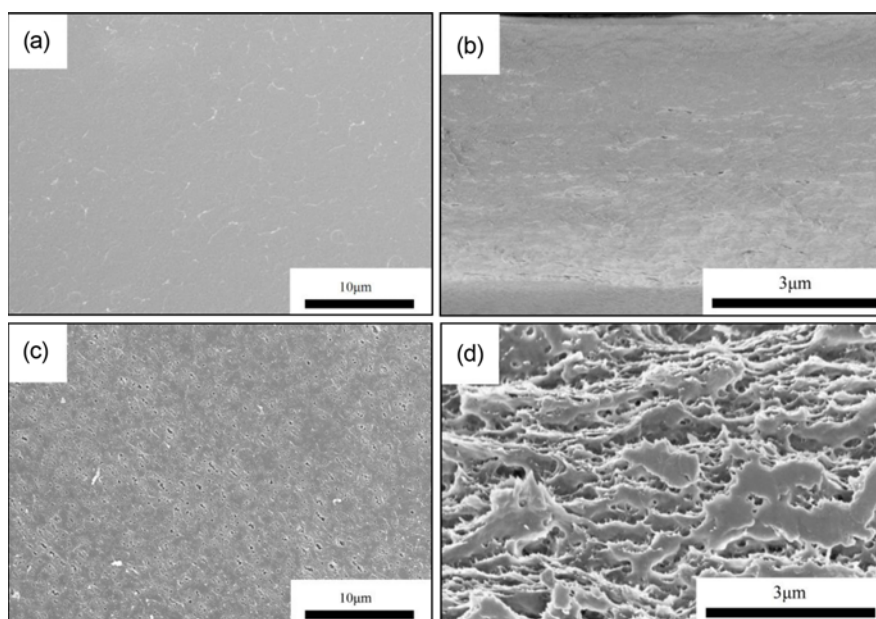


**Figure 6.** (a) SEM of BCM surface, (b) SEM of BCM cross-section, (c) SEM of BC-NFM surface, and (d) SEM of BC-NFM cross-section.

pore structure could be found on the surface of BCM. Figure 6(b) shows that the cross-sectional structure of BCM was also relatively dense. This is in agreement with the reported results [30]. BCM was modified to obtain BC-NFM; Figure 6(c) shows that obvious pores were observed on the surface. The cross-sectional image exhibits a spongy layered structure in BC-NFM, as shown in Figure 6(d). The FE-SEM analysis results indicate that hydrolysis and carboxymethylation have a significant effect on the surface and cross-sectional morphology structure of the BCM. This behavior may be attributed to strong molecular inter-atomic forces and hydrogen bonding in BCM; after modification, a part of the hydrogen bonding was changed into carboxymethyl, which disrupted the crystalline structures of the cellulose, and therefore, the internal structure became loose and an enhanced surface hydrophobicity was observed. Therefore, after modification, BCM has the function of nanofiltration.

### Carboxymethylation of the Hydrolyzed BCM

#### *Influence of Chloroacetic Acid Concentration to the Permeation Property of BCM*

There was no water flux of the BCM after hydrolysis, which happens peeling reaction in BCM. The Figure 7(a) and (b) show that the retention rate to NaCl and Na<sub>2</sub>SO<sub>4</sub> declines with increasing chloroacetic acid concentration. But water flux increases with increasing chloroacetic acid concentration. We speculate that the membrane surface can form the holes of nanofiltration level, and it has a certain retention performance to ion. When the concentration of chloroacetic acid is 3 wt/v.%, water flux reaches the maximum, later increases and then slightly declines. This is due to concentration of the chloroacetic acid solution is too high to increase acidity of the solution and thus reduces efficiency of carboxymethylation reaction, which the reaction was inhibited and influences the water flux.

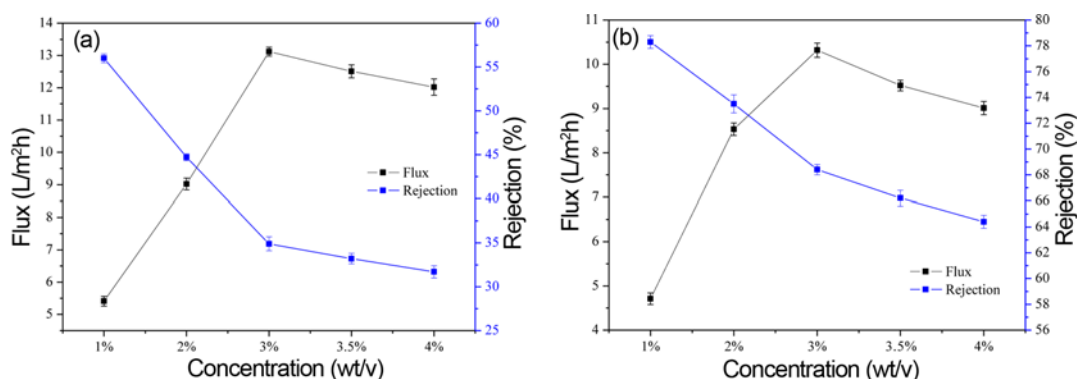


**Figure 7.** The influence of chloroacetic acid concentration to the performance of the BCM, (a) NaCl, (b) Na<sub>2</sub>SO<sub>4</sub>. Modification conditions: the reaction time was one hour, and the reaction temperature was 60 °C. Testing conditions employed were: 500 mg/l NaCl or Na<sub>2</sub>SO<sub>4</sub> solution as feed, the operating pressure was 0.5 MPa, room temperature solution.

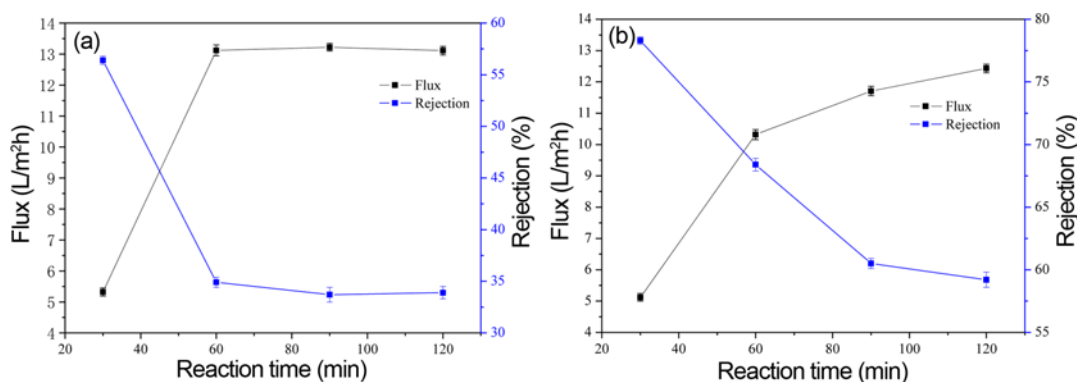


**Figure 8.** The influence of reaction time to the performance of the BCM, (a): NaCl, (b) Na<sub>2</sub>SO<sub>4</sub>. Modification conditions: concentration of chloroacetic acid was 3 wt/v.%, and the reaction temperature was 60 °C. Testing conditions employed were: 500 mg/l NaCl or Na<sub>2</sub>SO<sub>4</sub> solution as feed, the operating pressure was 0.5 MPa, room temperature solution.

#### ***Influence of Modification Time to the Permeation Property of BCM***

The Figure 8(a) and (b) show that the retention rate to NaCl and Na<sub>2</sub>SO<sub>4</sub> declines with increasing carboxymethylation reaction time. Water flux increases with increasing carboxymethylation reaction time. But the retention rate and water flux tends to be stable after 60 minutes. This is because the carboxymethylation reaction makes part of the hydrogen-based hydrolyzed membrane surface change into carboxymethyl, which is strong hydrophilic and having negative charges. Before 60 minutes, membrane surface will generate more carboxymethyl with increasing reaction time, and the hydrophilic, negative charge and permeation flux of membrane surface increases gradually. After the reaction carries out for 60 minutes, carboxymethylation reaction carries out completely. Membrane flux and retention rate keep stable. From the experimental, the best carboxymethylation reaction time was 60 minutes.

#### ***Influence of Different Operating Pressures to Water Flux and Rejection of BC-NFM***

Effect of operation pressure on the nanofiltration performance

of the BC-NFM was investigated with 500 mg/l NaCl and 500 mg/l Na<sub>2</sub>SO<sub>4</sub> solutions as feed, respectively, and the experimental results are shown in Figure 9. It was observed obviously that the water flux of the BC-NFM increased linearly with increasing the operating pressure. This is demonstrated that the BC-NFM was typical for most of the nanofiltration membrane. In addition, it was observed that the rejection of BC-NFM to NaCl and Na<sub>2</sub>SO<sub>4</sub> were decreasing but no significant change with increasing the operating pressure. It illustrates that the BC-NFM has good separation performance under range of certain operating pressure.

#### ***Molecular Weight Cut-off and Mean Pore Size of BC-NFM***

The molecular weight cut-off (MWCO) and pore size of the BC-NFM was determined through PEG retention tests. In this study, PEG was chosen since low interaction with the membrane material [31,32]. The corresponding MWCO curve was obtained from a plot of the rejection of different single-solutions of PEG versus their molecular weight (Figure 10). From the results it is seen the rejection increased

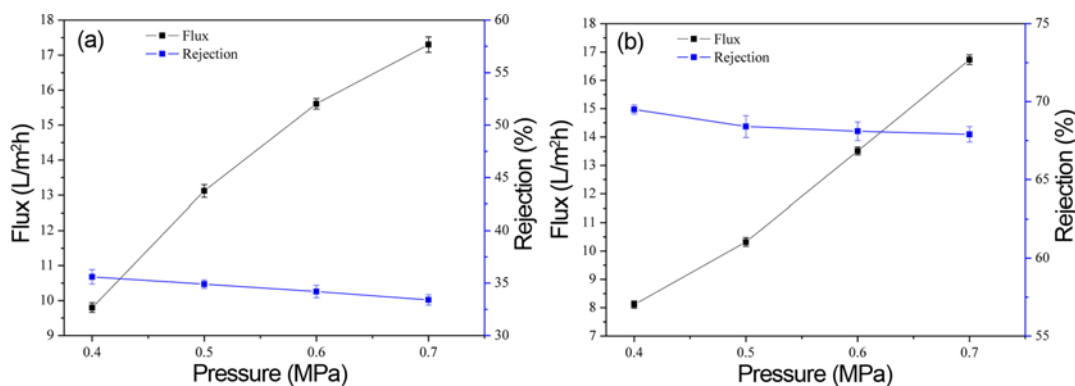


**Figure 9.** The influence of operating pressure to the performance of BC-NFM, (a) NaCl, (b) Na<sub>2</sub>SO<sub>4</sub>. Modification conditions: concentration of chloroacetic acid was 3 wt/v.%, the reaction time was one hour and the reaction temperature was 60 °C. Testing conditions employed were: 500 mg/l NaCl or Na<sub>2</sub>SO<sub>4</sub> solution as feed, the operating pressure was 0.5 MPa, room temperature solution.

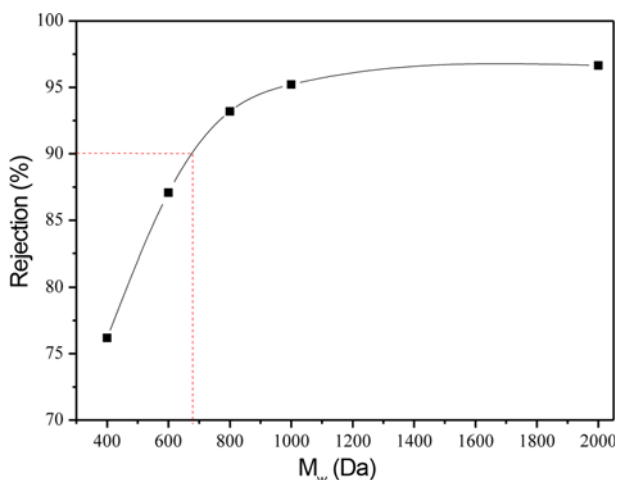


**Figure 10.** MWCO determination using PEG solutions. Modification conditions: concentration of chloroacetic acid was 3 wt/v.%, the reaction time was one hour and the reaction temperature was 60 °C. Testing conditions employed were: 100 mg/l PEG solutions as feed, the operating pressure was 0.5 MPa, room temperature solution.

with the molecular weight, as one would expect, the MWCO value was about 678 Da. Therefore, using the relationship between Stokes radius and MWCO, the Stokes radius of BC-NFM was calculated to be about 0.63 nm. The result illustrates that BC-NFM reached the nanofiltration level.

#### Treatment of Dye Aqueous Solutions

Using Methyl orange and methyl blue as models in nanofiltration interception test. The result of Figure 11 shows that the retention rate of BC-NFM to methyl blue is 98.9 %, and the water flux is 10.12 l/m<sup>2</sup>h. The retention rate of BC-NFM to methyl orange is 93.0 %, and the water flux is 12.31 l/m<sup>2</sup>h. The BC-NFM to two kinds of dyes has higher retention rate. Its separation effect to charged dye is affected by the screening effect and the Donnan effect together [33-

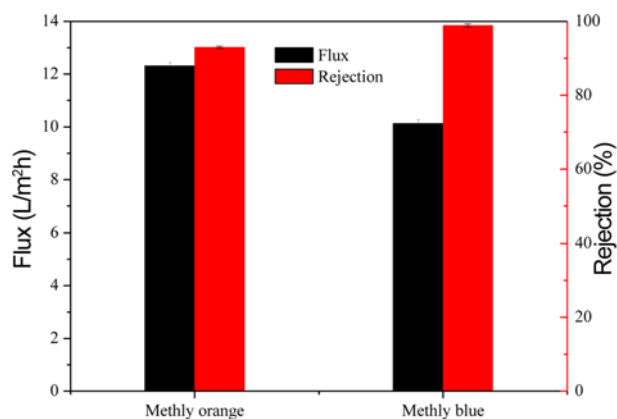


**Figure 11.** Dye retention rates and steady water fluxes of the BC-NFM in treatment of dye aqueous solution. Modification conditions: concentration of chloroacetic acid was 3 wt/v.%, the reaction time was one hour and the reaction temperature was 60 °C. Testing conditions employed were: 100 mg/l methyl orange or methyl blue dye solution as feed, the operating pressure was 0.5 MPa, room temperature solution.

35]. The molecular weight of the dye is larger, the negative charge carried by the dye is stronger, and the interception effect of membrane to the dye is better.

#### Conclusion

In this work, the modification of BCM for BC-NFM was investigated. The following conclusions can be drawn from the experimental results.

1. BC-NFM can be prepared by using NaOH hydrolysis and chloroacetic acid carboxymethyl modification to BCM. The study found that the membrane has best performance when concentration of chloroacetic acid was 3 wt/v.% and reaction 60 minutes. The BC-NFM with pore size of 0.63 nm has good performance for nanofiltration. At pressure of 0.5 MPa, the retention rate to NaCl and

Na<sub>2</sub>SO<sub>4</sub> were 68.4 % and 34.9 %, and the water flux were 10.32 l/m<sup>2</sup>h and 13.12 l/m<sup>2</sup>h, respectively. The retention rate to methyl orange and methyl blue were 93.0 % and 98.9 %, and the water flux were 12.31 l/m<sup>2</sup>h and 10.12 l/m<sup>2</sup>h, respectively.

- The degree of crystallinity decreases in BC dissolution process and hydrogen bonds of polymer molecules are opened, which destroy the crystalline structure of cellulose I. Thermal stability of BC, BCM and BC-NFM gradually decrease. After modification, the surface of BC-NFM can form holes, and the spongy internal produces. There are no significant differences between the structure of BC and BCM. However, BC-NFM had C=O absorption peak of carboxyl.
- The biodegradable, inexpensive and good separation performance of nanofiltration membranes will be widely used in water treatment, biotechnology, the food industry, and gas separation applications.

### Acknowledgments

The authors are grateful for the high technology industries project of Fujian Development and Reform Commission (2014, NO.514), China, and the Academy-Industry Cooperation Project of Industrial and University (2016H6004), Fujian Province, China.

### References

- N. Hilal, H. Al-Zoubi, N. A. Darwish, A. W. Mohammad, and M. Abu Arabi, *Desalination*, **170**, 281 (2004).
- J. Su, Q. Yang, J. F. Teo, and T. S. Chung, *J. Membr. Sci.*, **355**, 36 (2010).
- Z. Thong, Y. Cui, Y. K. Ong, and T. S. Chung, *ACS Sustain. Chem. Eng.*, **4**, 5570 (2016).
- Y. He, Y. P. Tang, and T. S. Chung, *Ind. Eng. Chem. Res.*, **55**, 12929 (2016).
- Y. Zhang, S. Zhang, J. Gao, and T. S. Chung, *J. Membr. Sci.*, **515**, 230 (2016).
- N. Bolong, A. F. Ismail, M. R. Salim, D. Rana, T. Matsuura, and A. Tabe-Mohammadi, *Sep. Purif. Technol.*, **73**, 92 (2010).
- T. Goma Bilongo, J. C. Remigy, and M. J. Clifton, *J. Membr. Sci.*, **364**, 304 (2010).
- D. Wang, K. Li, and W. K. Teo, *J. Membr. Sci.*, **162**, 211 (1999).
- S. M. Dutcak, M. W. J. Luiten-Olieman, H. J. Zwijnenberg, L. A. M. Bolhuis-Versteeg, L. Winnubst, M. A. Hempenius, N. E. Benes, M. Wessling, and D. Stamatialis, *J. Membr. Sci.*, **372**, 182 (2011).
- A. Pinkert, K. N. Marsh, S. Pang, and M. P. Staiger, *Chem. Rev.*, **109**, 6712 (2009).
- S. Zhu, Y. Wu, Q. Chen, Z. Yu, C. Wang, S. Jin, Y. Ding, and G. Wu, *Green Chem.*, **8**, 325 (2006).
- T. Heinze and T. Liebert, *Progr. Polym. Sci.*, **26**, 1689 (2001).
- T. Nishino, I. Matsuda, and K. Hirao, *Macromolecules*, **37**, 7683 (2004).
- S. L. Williamson, R. S. Armentrout, R. S. Porter, and C. L. McCormick, *Macromolecules*, **31**, 8134 (1998).
- K. J. Edgar, K. M. Arnold, W. W. Blount, J. E. Lawniczak, and D. W. Lowman, *Macromolecules*, **28**, 4122 (1995).
- J. F. Masson and R. S. John Manley, *Macromolecules*, **24**, 5914 (1991).
- J. F. Masson and R. S. John Manley, *Macromolecules*, **24**, 6670 (1991).
- K. Hattori, J. A. Cuculo, and S. M. Hudson, *J. Polym. Sci., Part A: Polym. Chem.*, **40**, 601 (2002).
- H. P. Fink, P. Weigel, H. J. Purz, and A. Bohn, *Recent Res. Devel In Polym. Sci.*, **2**, 387 (1998).
- M. J. Earle and K. R. Seddon, *Pure Appl. Chem.*, **72**, 1391 (2000).
- S. C. Yu, Q. B. Cheng, C. M. Huang, J. Liu, X. Y. Peng, M. H. Liu, and C. J. Gao, *J. Membr. Sci.*, **434**, 44 (2013).
- C. M. Shih, Y. T. Shieh, and Y. K. Twu, *Carbohydr. Polym.*, **78**, 169 (2009).
- Y. Z. Xu and R. E. Lebrun, *Desalination*, **122**, 95 (1999).
- X. L. Li, L. P. Zhu, B. K. Zhu, and Y. Y. Xu, *Separation and Purification Technology*, **83**, 66 (2011).
- M. Dalwani, N. E. Benes, G. Bargeman, D. Stamatialis, and M. Wessling, *J. Membr. Sci.*, **363**, 188 (2010).
- Q. Yang, T. S. Chung, and Y. E. Santoso, *J. Membr. Sci.*, **290**, 153 (2007).
- S. Lin, L. H. Chen, L. L. Huang, S. L. Cao, X. L. Luo, K. Liu, and Z. H. Huang, *Bioresources*, **7**, 5488 (2012).
- H. Zhao, J. H. Kwak, Y. Wang, J. A. Franz, J. M. White, and J. E. Holladay, *Energy Fuels*, **20**, 807 (2006).
- S. K. Mahadeva and J. Kim, *J. Phys. Chem. C.*, **113**, 12523 (2009).
- G. Arthanareeswaran, P. Thanikaivelan, K. Srinivasn, and M. Rajendran, *Eur. Polym. J.*, **40**, 2153 (2004).
- B. K. Barai, R. S. Singhal, and P. R. Kulkarni, *Carbohydr. Polym.*, **32**, 229 (1997).
- B. Vander Bruggen, J. Schaep, D. Wilms, and C. Vandecasteele, *J. Membr. Sci.*, **156**, 29 (1999).
- K. Y. Wang and T. S. Chung, *J. Membr. Sci.*, **247**, 37 (2005).
- C. G. Arlindo and C. G. Isolina, *J. Membr. Sci.*, **255**, 157 (2005).
- Y. C. Chung, N. D. Khiem, J. W. Choi, and B. C. Chun, *Fiber. Polym.*, **16**, 492 (2015).